



Seasonality of coastal upwelling trends in the Mauritania-Senegalese region under RCP8.5 climate change scenario

R. Vázquez^{a,c,*}, I.M. Parras-Berrocal^a, S. Koseki^b, W. Cabos^c, D.V. Sein^{d,e}, A. Izquierdo^a

^a Instituto Universitario de Investigación Marina (INMAR), Universidad de Cádiz, Spain

^b Geophysical Institute, University of Bergen, Bjerknes Centre for Climate Research, Norway

^c Departamento de Física y Matemáticas, Universidad de Alcalá, Spain

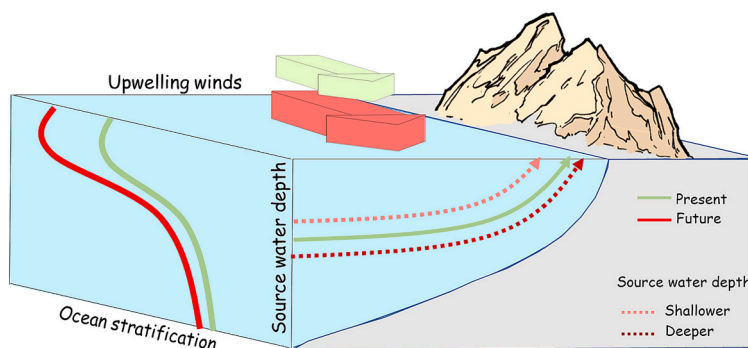
^d Alfred Wegener Institute for Polar and Marine Research, Germany

^e Shirshov Institute of Oceanology, Russian Academy of Sciences, Moscow, Russia

HIGHLIGHTS

- Mauritania Senegalese Upwelling in a high resolution regional climate system model
- The Azores high drives the intensification of upwelling favourable winds in the future.
- The role of the enhanced ocean stratification in the coastal upwelling
- Upwelling source depth affected by changes in wind and ocean stratification

GRAPHICAL ABSTRACT



ARTICLE INFO

Guest Editor: Jesús Forja

Keywords:

Coastal upwelling
Climate change
Ocean stratification
Upwelling favourable winds
Upwelling source water depth
Regional climate system model

ABSTRACT

The Mauritania-Senegalese upwelling region (MSUR), the southernmost region of the Canary current upwelling system, is well-known for its coastal productivity and the key role it plays in enriching the oligotrophic open ocean through the offshore transport of the upwelled coastal waters. The great ecological and socio-economic importance makes it necessary to evaluate the impact of climate change on this region. Hence, our main objective is to examine the climate change signal over the MSUR with a high resolution regional climate system model (RCSM) forced by the Earth system model MPI-ESM-LR under RCP8.5 scenario. This RCSM has a regional atmosphere model (REMO) coupled to a global ocean model (MPIOM) with high-resolution in the MSUR, which allows us to evaluate the wind pattern, the ocean stratification, as well as the upwelling source water depth, while maintaining an ocean global domain. Under RCP8.5 scenario, our results show that the upwelling favourable winds of the northern MSUR are year-round intensified, while the southern MSUR presents a strengthening in winter and a weakening in March–April. Along with changes in the wind pattern, we found increased ocean stratification in the spring months. In those months southern MSUR presents a shallowing of the upwelling source water depth associated to changes in both mechanisms. However, in winter the whole MSUR shows a deepening of the upwelling source water depth due to the intensification of the upwelling favourable

* Corresponding author at: Instituto Universitario de Investigación Marina (INMAR), Universidad de Cádiz, Spain.

E-mail address: ruben.vazquez@uca.es (R. Vázquez).

<https://doi.org/10.1016/j.scitotenv.2023.166391>

Received 27 April 2023; Received in revised form 13 August 2023; Accepted 16 August 2023

Available online 17 August 2023

0048-9697/© 2023 The Authors. Published by Elsevier B.V. This is an open access article under the CC BY-NC-ND license (<http://creativecommons.org/licenses/by-nc-nd/4.0/>).

winds, with the increased ocean stratification playing a secondary role. Our results demonstrate the need to evaluate the future evolution of coastal upwelling systems taking into account their latitudinal and seasonal variability and the joint contribution of both mechanisms.

1. Introduction

The Canary Current Upwelling System (CCUS) is one of the four large Eastern Boundary Upwelling Systems (EBUSs) sustaining a very fertile and productive marine ecosystem (Abrahams et al., 2021). EBUSs are driven by the equatorward alongshore winds that transport the surface waters offshore (Ekman dynamics), which in turn are replaced by cold and nutrient-rich waters from subsurface (Bakun, 1990).

CCUS is located in the eastern limb of the North Atlantic subtropical gyre (Kämpf and Chapman, 2016), extending from the northern tip of the Iberian Peninsula (43°N) to the southwest of Senegal (around 12°N). Although the CCUS is well known for its coastal productive areas, it also plays a key role in the enrichment of the oligotrophic open ocean through the shedding of mesoscale structures as filaments and eddies, which contribute to the offshore transport of the upwelled coastal waters (Lovecchio et al., 2017). In terms of seasonality and intensity, the CCUS is divided into four regions: Iberian upwelling region (35°N-43°N), weak permanent upwelling region (26°N-33°N), permanent upwelling region (21°N-26°N) and the southernmost Mauritania-Senegalese upwelling region (12°N-19°N; MSUR).

The MSUR, unlike the rest of the CCUS, is not only influenced by the Azores high pressure centre, but it is also highly dependent on the latitudinal migration of the Intertropical Convergence Zone (ITCZ) (Sylla et al., 2019). In winter, when the ITCZ reaches its southernmost position, the strong northeastern equatorward trade winds cause upwelling in the coast of Guinea, Senegal and Mauritania (12°N-19°N). However, in summer, the ITCZ shifts to the north, weakening the winds in the whole region. As a result the coastal upwelling is reduced, even reversing to downwelling in the Senegalese region (Cropper et al., 2014) due to the appearance of the onshore monsoonal winds (Gómez-Letona et al., 2017). Therefore, the MSUR presents a large seasonal and latitudinal variability clearly defined by the migration of the ITCZ (Pardo et al., 2011; Cropper et al., 2014; Benazzouz et al., 2015) and divided into two sub-regions by Cap Vert (~15°N), with year-round upwelling favourable winds in the northern MSUR and downwelling favourable winds during the summer months in the southern MSUR.

The future behavior of the EBUSs under climate change has been analyzed in a number of studies under different hypothesis and yielding different outcomes. As early as 1990, Bakun proposed that an increased warming over the continent in comparison to the ocean would result in a strengthening in upwelling favourable winds. Rykaczewski et al. (2015) proposed that the changes in the upwelling favourable winds would be mostly related to shifts in the position and timing of the high pressure cells rather than changes in the continental thermal low pressure systems. Sylla et al. (2019) bore out this hypothesis for the MSUR, where they found a strong relationship between changes in the upwelling and shifts in the Azores high along with an influence of the Sahara thermal low expansion in the northern MSUR. However, the wind is not the only driver of change at the end of the 21st century and Oyarzún and Brierley (2019) and Sousa et al. (2020) found that global warming could cause an increase in the ocean stratification that will disconnect the wind stress from the deeper waters.

However, the coarse spatial resolution (below 1° x 1°) of GCMs comprised in CMIP5 is not enough to resolve the latitudinal EBUS variability and to reproduce their mesoscale features or detailed shelf dynamics (García-Reyes et al., 2015; Xiu et al., 2018; Varela et al., 2022). Thus, there is still uncertainty about what is the main driver of future change in the MSUR, and the relative roles played by the ocean stratification and wind. Although the models from High Resolution Model Intercomparison project (HighResMIP, Haarsma et al., 2016)

present an opportunity for nearshore analysis (Varela et al., 2022; Sylla et al., 2022) they still have a resolution coarser than 25 km. In fact, recent studies (García-Reyes et al., 2015; Wang et al., 2015a, 2015b; Sein et al., 2017; Gómez-Letona et al., 2017; Bindoff et al., 2019; Vázquez et al., 2022) showed the need for much higher horizontal resolution for the representation of mesoscale processes in the upwelling systems that are partly masked in the current GCMs. Considering the increased upper-ocean stratification and decreased nutrient supply, exploring the response of ecosystems to intensified upwelling and ocean surface warming would require a more detailed modeling framework for a better representation of the relevant physical processes. Regional Climate Systems Models are able of reproducing such physical processes (RCSMs) (Xiu et al., 2018; Vázquez et al., 2022).

The MSUR is considered to be the most productive region in the CCUS, according to Aristegui et al. (2009). However, the attempt to evaluate the effects of climate change has triggered a significant amount of uncertainty due to the coarse resolution of GCMs. Therefore, this study aims to investigate the evolution of the MSUR under the RCP8.5 scenario with a RCM that is capable of reproducing the relevant mesoscale processes in the other three CCUS regions with high confidence for the present climate conditions (Vázquez et al., 2022).

The objectives of this study can be summarized as follows:

- First, to validate the representation of the main variables in the MSUR for the present climate.
- Second, to assess the projected climate change signal in the MSUR under the RCP8.5 scenario, analyzing both the effects of the wind pattern and the ocean stratification changes under the global warming conditions.

The paper is organized as follows: the model, data sets and methodology are described in Section 2, the model validation and the results are presented in Sections 3 and 4, respectively. Finally, the discussion is presented in Section 5 and conclusions are presented in Section 6.

2. Material and methods

2.1. Model setup

In this study we use the RCM ROM (Sein et al., 2015), which comprises the REgional atmosphere MOdel REMO (e.g. Jacob, 2001) with horizontal resolution of 25 km with a rotated grid coupled to the global ocean-sea ice-marine biogeochemistry model MPIOM/HAMOC (Marsland et al., 2003) via the OASIS3 coupler (Valcke, 2013). Moreover, ROM includes the Hydrological Discharge model (Hagemann and Dumenil-Gates, 1998, 2001) and a dynamic/thermodynamic sea ice model (Hibler, 1979).

MPIOM is discretized on an orthogonal curvilinear Arakawa C-grid, with two grid poles over North America and northwestern Africa that allows a high resolution in the CCUS while maintaining a global domain (Vázquez et al., 2022). In the MSUR, the MPIOM resolution ranges from 9 km (northernmost region) to 15 km in the southernmost region (Fig. 1). The ocean model has 40 vertical levels with increasing level thickness towards the ocean bottom (Sein et al., 2015; Vázquez et al., 2022). The ocean spin-up was done according to the procedure described in Sein et al. (2015). MPIOM is started with climatological temperature and salinity data (Levitus et al., 1998). Subsequently, it is integrated six times through the 1958–2002 period forced by ERA-40 and one more time by ERA-Interim reanalysis (1979–2012) and with 60 min coupling timestep.

In this work we use two different global sources to provide lateral boundary conditions for REMO and to force MPIOM outside the coupling region: ERA-Interim (Dee et al., 2011) and MPI-ESM-LR (Giorgetta et al., 2013). In the region covered by REMO (Fig. 1) the atmosphere and the ocean interact while prescribed atmospheric forcing drives the rest of the global ocean, outside the coupled domain. A 30 year-long experiment forced by ERA-Interim (ROM_P0) was used to evaluate the ability of ROM to simulate the present climate (1980–2012) in the MSUR. Then, in order to evaluate the impact of climate change in the MSUR, we run ROM model forced by MPI-ESM-LR (about 1.5° ocean and 2° atmospheric resolution) for two periods: the first, extends from 1950 to 2005 (ROM_P1) is the historical run and the second, which extends from 2006 to 2099 represents the future climate under the Representative Concentration Pathway 8.5 (RCP 8.5) CMIP5 scenario (ROM_P2), which is the most unfavourable scenario in terms of greenhouse gas emissions.

2.2. Study area

Our study area, MSUR, is defined by the separation of the Canary current from the coast in Cape Blanc (21°N; Stramma, 1984) at the north and by the southern limit of the winter/spring upwelling favourable winds at Cape Roxo (12°N; Capet et al., 2017). The upwelling favourable winds strongly depend on the latitudinal at migration of the ITCZ, leading to significant seasonal variability (Sylla et al., 2019). As a result the highest chlorophyll concentrations are found during the upwelling season (winter/spring), presenting a drastic decrease during the summer season with the relaxation of the wind-driven upwelling (Lathuilière et al., 2008).

During the upwelling season, a poleward undercurrent develops, as is also observed in other upwelling systems (Kounta et al., 2018), at depths ranging from 100 to 200 m (Vélez-Belchí et al., 2021). However,

in the MSUR, this poleward undercurrent differs from other EBUSs (Capet et al., 2017), since it intensifies in the surface layers during the summer months when the upwelling favourable winds relax (Peña-Izquierdo et al., 2012). This surface countercurrent is referred to as the Mauritanian Current (MC; Kirichek, 1971). While there is a debate whether the MC differs from the poleward undercurrent or not (Barton, 1998; Kounta et al., 2018), what is certain is that it leads to a 2.5-fold increase in northward flow during summer compared to the upwelling season, transporting waters of mainly South Atlantic origin into the MSUR (Klenz et al., 2018). Therefore, based on its seasonal characteristics, the MSUR can be divided into two sub-regions with differences in atmospheric forcings, ocean conditions, and shelf/slope morphology: the northern MSUR (15–19°N) and the southern MSUR (12–15°N; Capet et al., 2017).

The MSUR stands out due to a remarkably strong seasonal sea surface temperature (SST) cycle compared to similar latitudes in the open ocean (Mignot et al., 2020), and its annual cycle is displaced relative to the wind field, with maximum SST occurring during the summer months (Pardo et al., 2011). In general, mesoscale processes such as filaments are identified in EBUSs as a cross-shore elongation in the SST field from coast to open sea (Santana-Falcón et al., 2020). However, in MSUR, it is found a cold tongue that extends latitudinally, from Cap Vert to the south even to 12°N. This is mainly due to the very shallow shelf of the southern MSUR, with depths below 30 m in the first 50 km of the shelf. This results in the overall orientation of the cold tongue being north-south, remaining stable for days and weeks, and ultimately delaying the export of water masses from the shelf to the open sea (Capet et al., 2017).

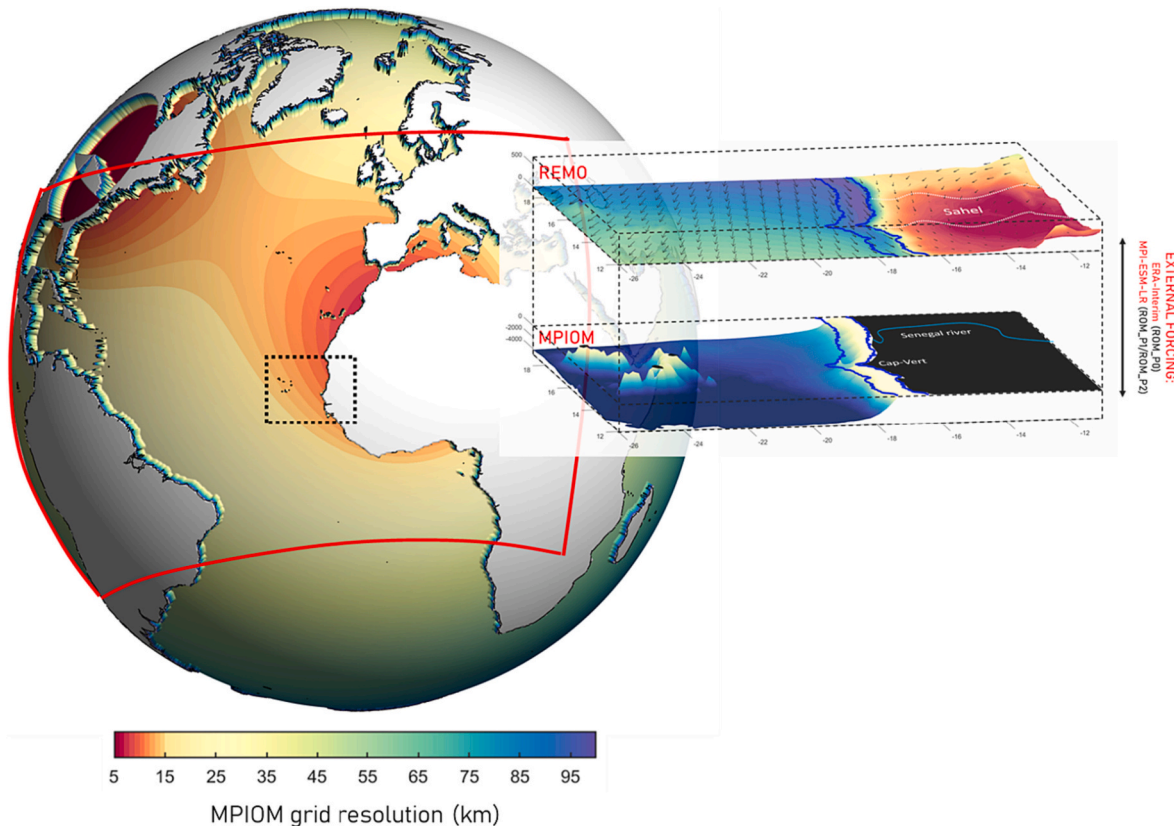


Fig. 1. MPI-OM grid resolution (km) and REMO domain (red line). The black box represents the MSUR domain (12°N–19°N). The overlaid figure outlines the MSUR domain with the external forcing and the mask used for the upwelling index calculation (blue lines). It is also outlined the 2 m air temperature, the wind field, and the model bathymetry and topography. The Sahel region was located following Ikazaki (2015).

2.3. Validation strategy and climate change evaluation

To evaluate the ROM_P0 performance in the MSUR, we focus on the wind field over the coastal band from which we build an upwelling index (Eq. (3)). We also evaluate the main drivers involved in the changes of upwelling winds over the MSUR: Azores high and the ITCZ. The validation is carried out against ERA5 reanalysis (Hersbach et al., 2020), which presents a constant spatial resolution of 31 km.

The upwelling index (UI , Bakun, 1973) is based on the offshore wind-driven Ekman transport (Q) and is calculated as follows:

$$Q_x = \frac{\tau_y}{f\rho_0} \quad (1)$$

$$Q_y = -\frac{\tau_x}{f\rho_0} \quad (2)$$

$$UI = -\sin\left(\theta - \frac{\pi}{2}\right)Q_x + \cos\left(\theta - \frac{\pi}{2}\right)Q_y \quad (3)$$

where Q_x , Q_y and τ_x , τ_y are the zonal and meridional components of the horizontal Ekman transport and the wind stress vector, respectively; ρ_0 is the reference sea water density (1025 kg m^{-3}); f is the Coriolis parameter and θ is the angle between the coastline and the equator. The UI is estimated within a 100 km wide band along the MSUR (mask in Fig. 1; Benazzouz et al., 2014; Lovecchio et al., 2017; Bonino et al., 2019) and it is expressed as the oceanward flow of surface waters per km of coastline ($\text{m}^3 \text{ s}^{-1} \text{ km}^{-1}$; Pardo et al., 2011). The Azores high and the ITCZ position are assessed from the mean sea level pressure (MSLP) and wind fields.

In order to assess the future change in seasonality and intensity of the coastal upwelling we use the whole historical (1950–2005) and RCP8.5 (2006–2099) simulated periods to calculate the UI , near-surface air temperature (T2m) and MSLP trends. Also, we calculate the wind change as the difference between the time-averaged ROM_P2 (2070–2099) and ROM_P1 (1976–2005) outputs. Moreover, the coastal stratification is characterized in both periods through the Brunt-Väisälä frequency (N), where larger values indicate strong stratification, and values close to zero a well-mixed water column:

$$N^2 = \frac{g}{\rho_0} \frac{\partial \rho}{\partial z} \quad (4)$$

where z is the depth, ρ the potential density and g is the gravitational acceleration.

We also use the source depth (D_s) to estimate the depth of the waters that reach the surface in the coastal upwelling region. D_s gives us further insight into the properties of upwelled waters and the mechanisms that drive the coastal upwelling in the future, as a combined effect of the changes in wind stress and coastal ocean stratification. This parameter is defined in He and Mahadevan (2021) as follows:

$$D_s = C_s \sqrt{\frac{UI}{N}} \quad (5)$$

where $C_s = (4/C_e)^{1/2} = 8.16$ for $C_e = 0.06$, which is the efficiency factor used in Fox-Kemper et al. (2008) and He and Mahadevan (2021).

In this context, there are different methods to identify the source depth with more accuracy, such as using Lagrangian particles (e.g. Capet et al., 2004; Oerder et al., 2015; Ndoye et al., 2017) or the concentration of passive tracers (e.g. Izquierdo and Mikolajewicz, 2019) as source water markers. However, the time resolution of our model output is too low to apply such approaches offline. Therefore, we resorted to this diagnostic to assess the source depth, which is simpler but provides useful information.

3. Evaluation

3.1. Alongshore winds

In terms of the UI , the MSUR is divided in two parts: The northern MSUR extends from the south of Cape Blanc (19°N) to Cap Vert (15°N), where the UI is positive year-round, with peaks in April and May (Fig. 2a). The southern MSUR is located to the south of 15°N , where the coastal ocean is under downwelling favourable winds from July to September, as the ITCZ reaches its northernmost position in summer.

ROM_P0 reproduces well the seasonal cycle of the UI (Fig. 2b), presenting the same seasonal and spatial pattern as ERA5, with the northward migration of the ITCZ in the summer period. ERA5 presents larger UI values than ROM_P0 in the northern MSUR from April to May (Fig. 2c). In summer, ROM_P0 presents a downwelling more extended to the north and intense than ERA5 ($-200 \text{ m}^3 \text{ s}^{-1} \text{ km}^{-1}$; Fig. 2c). These discrepancies may be partially explained by the improvement associated with the ocean-atmosphere coupling and the surface current velocity feedback in the wind stress, as well as by the higher horizontal resolution that presents ROM against ERA5. Coupling and a SST higher horizontal resolution allow a better representation of the North African Coastal Low Level Jet (Soares et al., 2019), which is a key pattern of the surface wind field along the North African coast. In this context, Vázquez et al. (2022) found significant differences in SST at the CCUS coastal band when comparing ERA5 reanalysis to the higher-resolution ESA observational dataset (Merchant et al., 2019), demonstrating the importance of high resolution to reproduce the mesoscale processes in the upwelling regions. Nevertheless, both the latitudinal and seasonal correlations between ERA5 and ROM_P0 winds are higher than 0.94, showing good abilities in reproducing the coastal wind field (Fig. S1).

3.2. Drivers of the alongshore winds

In this section we evaluate the drivers involved in the seasonal march of the alongshore favourable winds over the MSUR: The Azores high and the ITCZ. Both drivers present a seasonal north-south oscillation, since are part of the Hadley cell.

In April, the centre of the Azores high is located to the south of 35°N in ERA5, reaching its annual southernmost and easternmost position (Fig. 3a). These conditions make April the month with the strongest upwelling favourable winds in the MSUR. Moreover, along with the southward shift of the Azores high, the ITCZ presents its southernmost position, which is identified by surface winds convergence and associated with a low pressure band (between 5°S and 5°N). As a result there are upwelling favourable winds both in the northern and southern MSUR.

During the summer season, the Azores high and ITCZ shift to the north being located at 35°N and 13°N , respectively (Fig. 3d). This fact makes August the month with the weakest upwelling favourable winds in MSUR in the year, with downwelling favourable winds in the southern MSUR. ROM_P0 reproduces properly the seasonality of the MSLP field, representing the northward migration of the trade winds belt (Fig. 3e) and showing differences below 2 hPa both in April and August (Fig. 3c and f). Therefore, we can conclude that ROM is able to reproduce the main drivers of the wind field and its seasonality in the MSUR.

4. MSUR under global warming

With the objective to investigate possible seasonality changes in the MSUR for the future, we calculate the monthly UI trends (1950–2099) along the coast (Fig. 4). In January positive UI trends are found in the whole MSUR (Fig. 4a) with maximum values between 13°N and 15°N ($20 \text{ m}^3 \text{ s}^{-1} \text{ km}^{-1} \text{ decade}^{-1}$), due to a future strengthening of the upwelling favourable winds. From February to April (Fig. 4b-d) positive trends are found through all the northern MSUR, but the trends turn negative in the southern MSUR reflecting a weakening of the upwelling

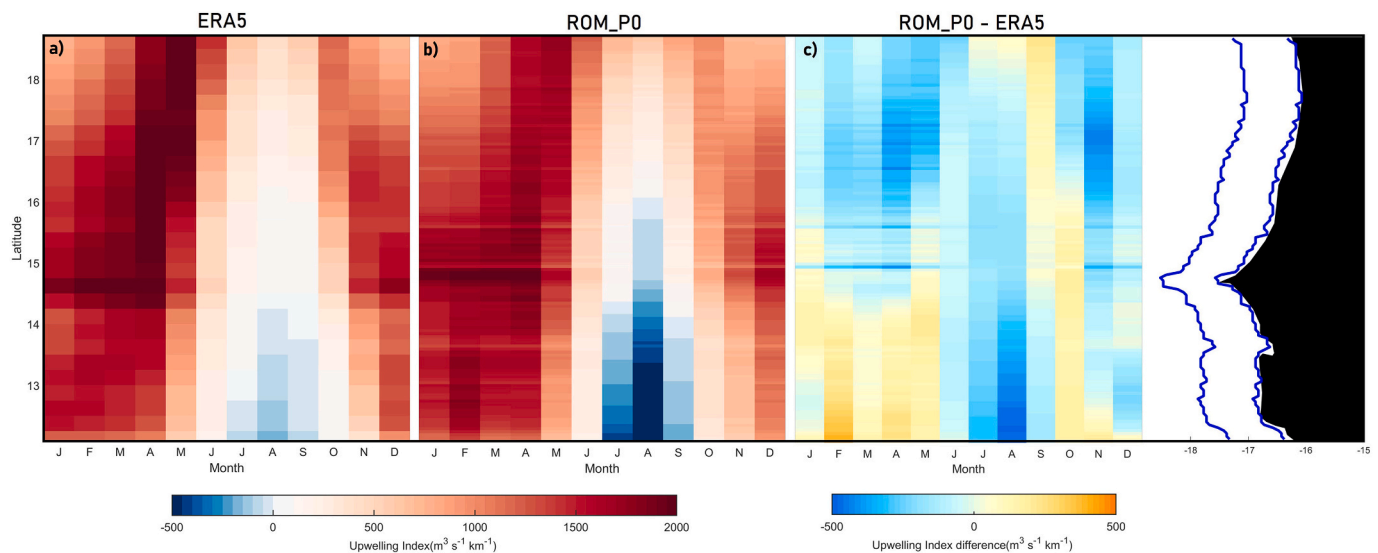


Fig. 2. Seasonal cycle of the UI ($m^3 s^{-1} km^{-1}$) averaged over the closest grid points to the coast in ERA5 (a), ROM_P0 (b) and the differences between ROM_P0 and ERA5 (c).

favourable winds ($-20 m^3 s^{-1} km^{-1} decade^{-1}$). In May (Fig. 4e) the UI trend is nearly zero in all MSUR. From June to September (Fig. 4f-i), the UI trends indicate a future intensification of the upwelling favourable winds for the northern MSUR and a weakening of the downwelling favourable winds in the southern MSUR (Fig. 2). In November–December (Fig. 4k-l), the trends are similar to January, positive in the whole region except for the southernmost latitudes. In order to assess the robustness of the obtained upwelling trends, we also calculated the trends using the Coastal Upwelling Transport Index (CUTI, Jacox et al., 2018), which is similar to UI in the sense that it estimates of the rate of vertical volume transport and has the same units. However, CUTI incorporates improved estimates of the Ekman transport and accounts for cross-shore geostrophic flow associated with an alongshore SSH gradient. The results show the same pattern of change as UI trends despite small latitudinal differences (Fig. S2).

On the basis of the UI trend latitudinal pattern we divide the year in three periods: (Period 1) January, November and December presenting positive trends over most of the region, with maximum values around $15^\circ N$ and negative trends in the southernmost region; (Period 2) March and April with bipolar UI trends: positive north of $15^\circ N$ and negative to the south; and (Period 3) June, July, August and September with positive UI trends in the whole domain. February, May and October were removed from the analysis because they behave as transition months between periods with clearly defined latitudinal patterns.

Along with the UI , we assessed the MSLP and T2m trends over the same period. In Period 1, when positive UI trends (Fig. 5a; black line) can be found in practically the whole coastal region with maximum values around Cap Vert, the T2m shows a remarkable local increase in the southern Sahel, around $12^\circ N$ – $14^\circ N$, while the Azores high intensifies (Fig. 5c). These conditions strengthen the upwelling favourable winds over the whole MSUR. Moreover, the local increase of T2m in the southern region of Sahel reduces the continental low pressures, generating a cyclonic circulation anomaly around $15^\circ N$ and $12^\circ W$. This mechanism further intensifies the upwelling favourable winds in practically the whole domain, excepting $12^\circ N$, where the wind anomaly turns onshore, weakening the upwelling winds in the southernmost region (Fig. 5c; see with detail in Fig. S1a).

Period 2, similarly to Period 1, presents an increase in the MSLP at the Azores high. As the T2m increase over land is generally stronger than in Period 1, the decrease in MSLP is stretched out over the African continent (Fig. 5d–e). Therefore, the cyclonic circulation anomaly presents its core north of $15^\circ N$ and further east than in the Period 1,

intensifying the upwelling favourable winds (along with the Azores high strengthening) over the northern MSUR and to a weakening of the upwelling favourable winds in the southern MSUR (Fig. 5a; green line). Finally, Period 3 is dominated by the Sahara thermal low in summer, presenting a drastic increase of the T2m ($0.5^\circ C decade^{-1}$) in the African continent (Fig. 5f–g). Unlike the rest of periods, the Azores high does not present changes in intensity. The Saharan thermal low is located far away from the coastal region, so that the wind anomaly results with southeastern direction, stimulating slightly the upwelling favourable winds in the northern MSUR and weakening the downwelling winds in the southern MSUR.

Ocean stratification changes in the MSUR are evaluated with the help of the Brunt-Väisälä frequency. Brunt-Väisälä frequency is calculated within a 100 km wide band along the MSUR (the mask is shown in Fig. 6d) and averaged from surface to 150 m (the average depth associated with the ascent of water masses to the surface; Kämpf and Chapman, 2016). This analysis is realized for the three periods defined above.

For all periods the Brunt-Väisälä frequency is below $0.02 s^{-1}$ (Fig. 6a–c, red shading), with increasing values as latitude decreases. This is related to the influence of the warmer surface equatorial waters in the southern MSUR. The Period 3 presents the most stratified water column in the whole MSUR, associated with higher sea surface temperature in the summer season (Fig. 6c). Low values of the Brunt-Väisälä frequency are associated with a vertically homogeneous water column, in this case due to the coastal upwelling (strongest in Period 2).

In order to assess the changes in ocean stratification in the future we analyze the differences between ROM_P2 and ROM_P1 (Fig. 6; grey shading). In Period 1, we found a slight decrease in the ocean stratification in some region of the northern MSUR (Fig. 6a). This decrease is associated with a larger increase of the temperature in the sub-surface waters (50–70 m) than in the surface waters (Fig. S2a). In the Period 2 the ocean stratification increases in the whole MSUR, being more evident from $12^\circ N$ to $16^\circ N$. In Period 3 the stratification changes are similar to Period 2.

A very important characteristic of the upwelling is the source water depth. The upwelling source water depth is calculated in a simple way (see Eq. (5)) taking into consideration both the action of the alongshore favourable winds and the ocean stratification.

For the historical simulation (ROM_P1), in Period 1 the upwelling source water depth is around 60 m in the whole MSUR, with slightly larger values in the northern MSUR (Fig. 7a). The upwelling source

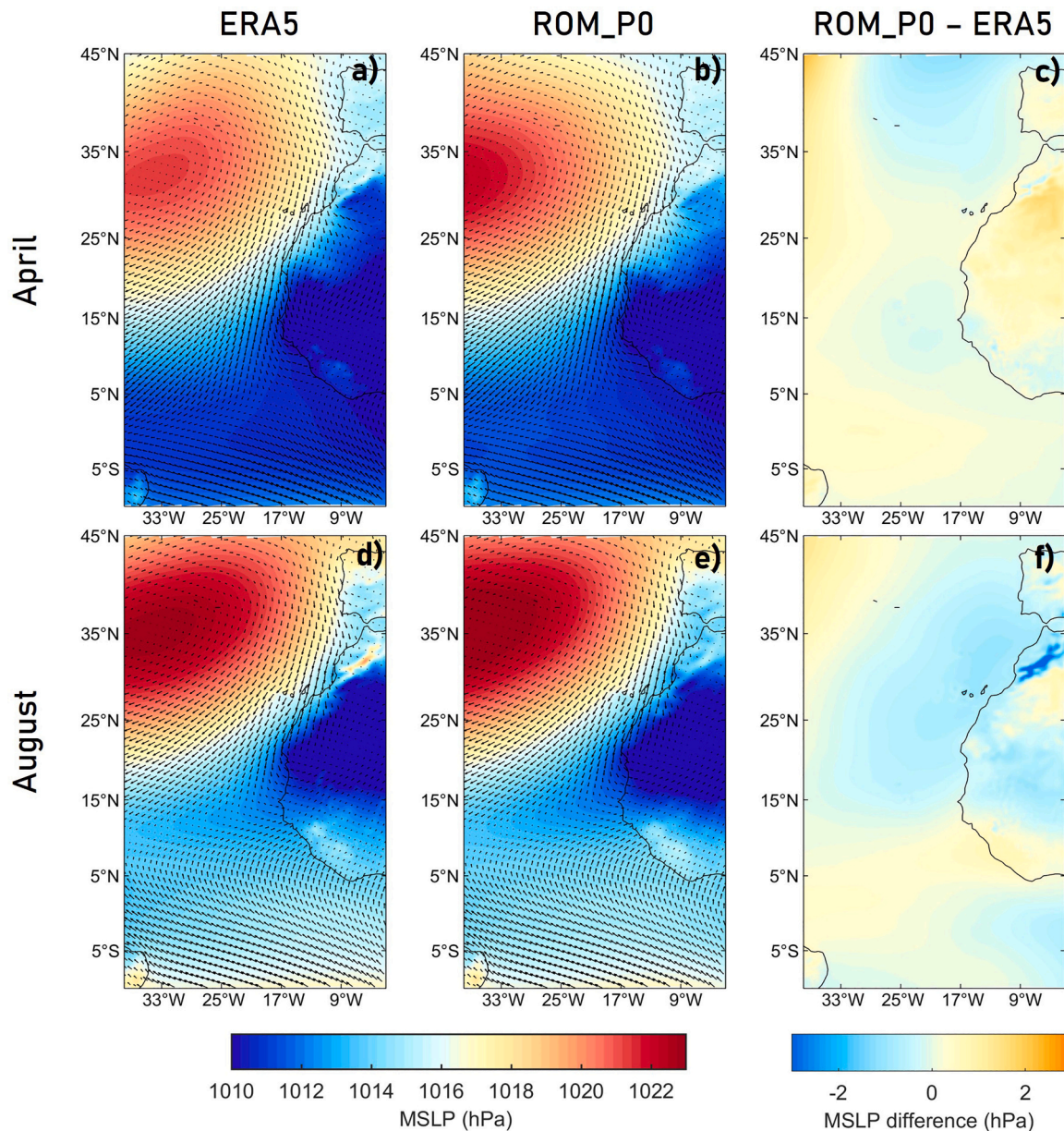


Fig. 3. Climatological mean sea level pressure (hPa) and wind field in April (top) and August (bottom) for ERA5 (a, d), ROM_P0 (b, e) and the differences between ROM_P0 and ERA5 (c, f) from 1980 to 2012.

water in Period 2, comes from ca. 80 m and deeper (around 90 m) in northern than in southern MSUR (Fig. 7c). Deeper sources are mainly associated with the strengthening of the upwelling favourable winds in this period. In Period 3 the maximum source water depth (ca. 70 m) is found at northernmost MSUR, and then linearly decreases to Cap Vert (30 m). To the south of Cap Vert the MSUR is dominated by downwelling favourable winds therefore there is no source water depth (Fig. 7e).

Differences in source water depth between ROM_P2 and ROM_P1 are shown in Fig. 7 (depicted in grey shading). The upwelling source water is deeper in ROM_P2 during Period 1 (approximately 5 m), and decreases towards the southernmost region. In Period 2, deeper sources are found in the northern MSUR and shallower sources from Cap Vert to the southernmost MSUR. The upwelling source water depth does not significantly change in the entire MSUR during Period 3.

5. Discussion

The impact of climate change on upwelling systems has been a topic

of interest over the last few decades. Both reanalysis and climate models have been used with the objective of understanding the impact of climate change on these important and productive ecosystems (Abrahams et al., 2021). However, the spatial resolution of the GCMs used for global climate projections is insufficient to adequately reproduce the upwelling systems, resulting in uncertainty in future projections. Here, we take advantage of the ROM RCM, which can reproduce the characteristics, variability, and associated mesoscale processes of the CCUS with high confidence (Vázquez et al., 2022). We investigate the future evolution of the MSUR under the RCP8.5 CMIP5 scenario using ROM driven by MPI-ESM-LR. We are aware that relying on a single model with only a forcing imposes limitations to the generalization of our results, however we are confident that they are a good basis for exploring these mechanisms in future studies with a larger number of drivers and regional climate models.

To date, the efforts of the scientific community to evaluate the effect of climate change on EBUSs have focussed on two different responses: changes in wind patterns (Varela et al., 2015; Sousa et al., 2017a; Sousa

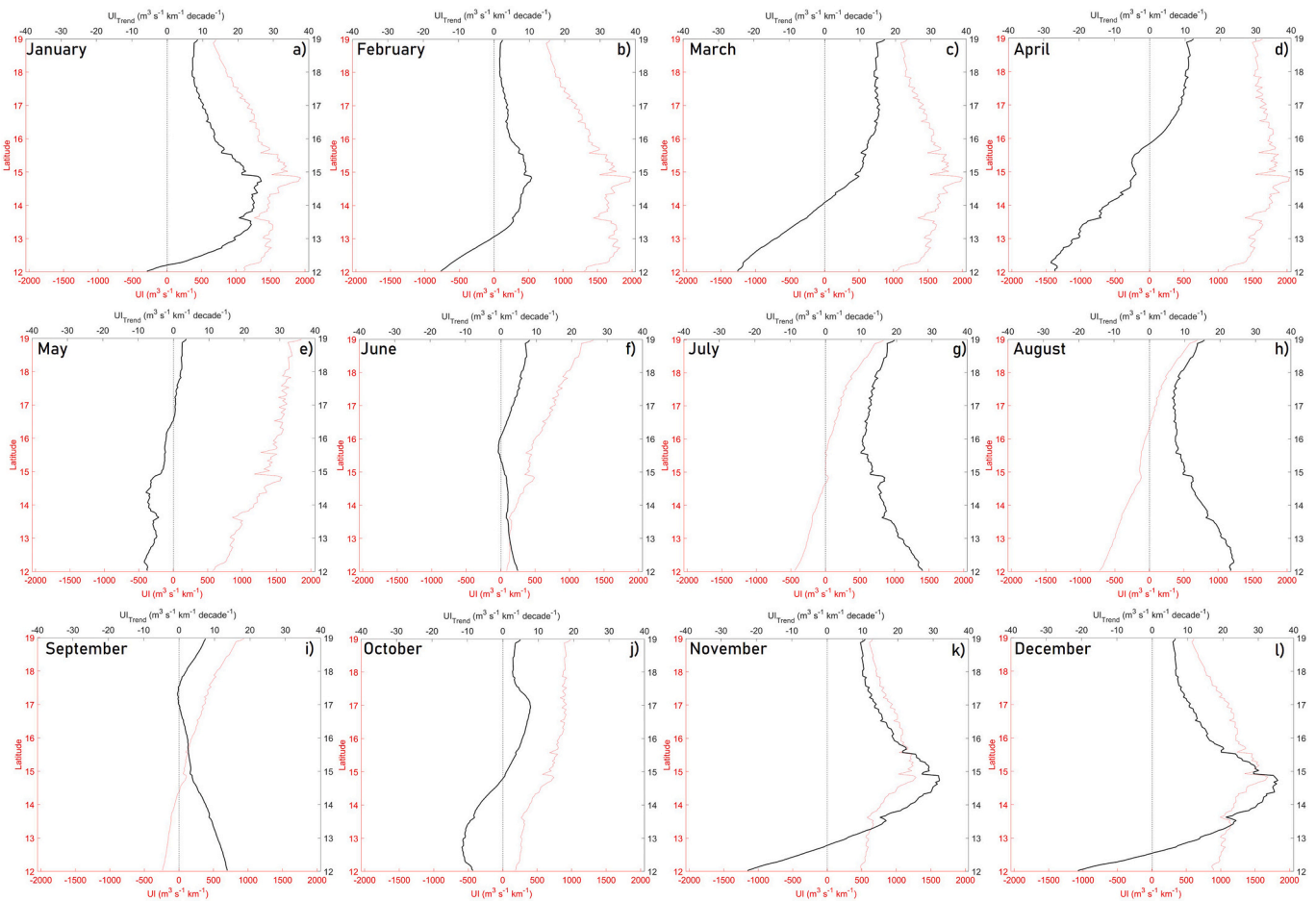


Fig. 4. Monthly linear trends of UI ($m^3 s^{-1} km^{-1} decade^{-1}$; black line) averaged over the closest grid points to the coast from 1950 to 2099. It is also added in red line, the UI averaged over the closest grid points to the coast of ROM_P0.

et al., 2017b; Sylla et al., 2019) and changes in ocean stratification (Oyarzún and Brierley, 2019; Sousa et al., 2020). Although both responses can provide useful information on the future of these ecosystems, obtaining a joint response from both mechanisms becomes essential. Recent studies have attempted to address the impact of climate change by combining both mechanisms using a large ensemble of the Community Earth System Model (Chang et al., 2023; Jing et al., 2023), conducting a joint study of the four main EBUSs. However, the large latitudinal and seasonal variability observed in our study, for a single region of the CCUS, indicates the difficulties of proposing a generic response for an entire upwelling system.

In fact, in this study we propose a monthly analysis of the UI trends to evaluate the effect of climate change on the MSUR, due to its large seasonal and latitudinal variability (Pardo et al., 2011; Cropper et al., 2014; Benazzouz et al., 2015). This analysis allowed us to find the causes of the changes in wind pattern throughout the year, identifying three periods with similar trends (Fig. 4). Sylla et al. (2019) proposed to evaluate the MSUR from November to May, as most studies associated with upwelling are only focused on the summer season, when the MSUR exhibits its weakest upwelling compared to other regions of the CCUS. They linked a weakening of the upwelling favourable winds in the southern MSUR (from Cap Vert to $12^\circ N$), to shift of the Azores High (Ryckaczewski et al., 2015). These results were compared with the trends of CUTI in Fig. S2, showing the same month clustering as found using UI . Furthermore, we also evaluated the trends in upward mass transport at the mixed layer depth using the model vertical velocity (not shown) to compare them with the UI and CUTI, revealing divergent trends in some months, as well as a larger latitudinal variability. Such differences in

estimates of upward mass transport and UI have also been reported by Sylla et al. (2019) and Jing et al. (2023). In this context, the increase in resolution plays a crucial role in understanding the effects of processes related to more accurate representation of the cross-shore wind stress, the coastline, the seafloor topography and ocean mesoscale structures, presenting a challenge for HighResMIP and coupled regional models to identify the role of these processes in EBUSs.

Our results in two out of the three annual periods are in agreement with this hypothesis for the MSUR. We detected a strengthening of the Azores high (Ryckaczewski et al., 2015; Sousa et al., 2017a, 2017b; Sousa et al., 2017b; Aguirre et al., 2019; Sylla et al., 2019; Varela et al., 2022), which strengthens the upwelling favourable winds in the Periods 1 and 2. However, our monthly UI trends analysis suggests that other processes also affect the change in upwelling favourable winds in MSUR: during Period 1 the MSUR upwelling is enhanced by a strong T2m local increase over the southern region of Sahel that can be explained by a southward expansion of the Sahara desert (e.g., Cook and Vizy, 2015; Zhou, 2016). In this context, we find that the local T2m changes have a remarkable impact on the upwelling favourable winds unlike Period 2 (see with detail in Fig. S1). During the summer months (Period 3), there are not significant changes in position or intensity of the Azores high. Nevertheless, we detected an evident increase in the T2m land-sea differences associated to an intensification of the Saharan thermal low that leads to a southeastern wind anomaly (e.g., Bakun, 1990), which reinforce slightly the upwelling favourable winds over the northern MSUR and weakens the downwelling favourable winds in the southern MSUR.

Oyarzún and Brierley (2019) found that the increase in the stratification of the upper layers of the water column in the Humboldt

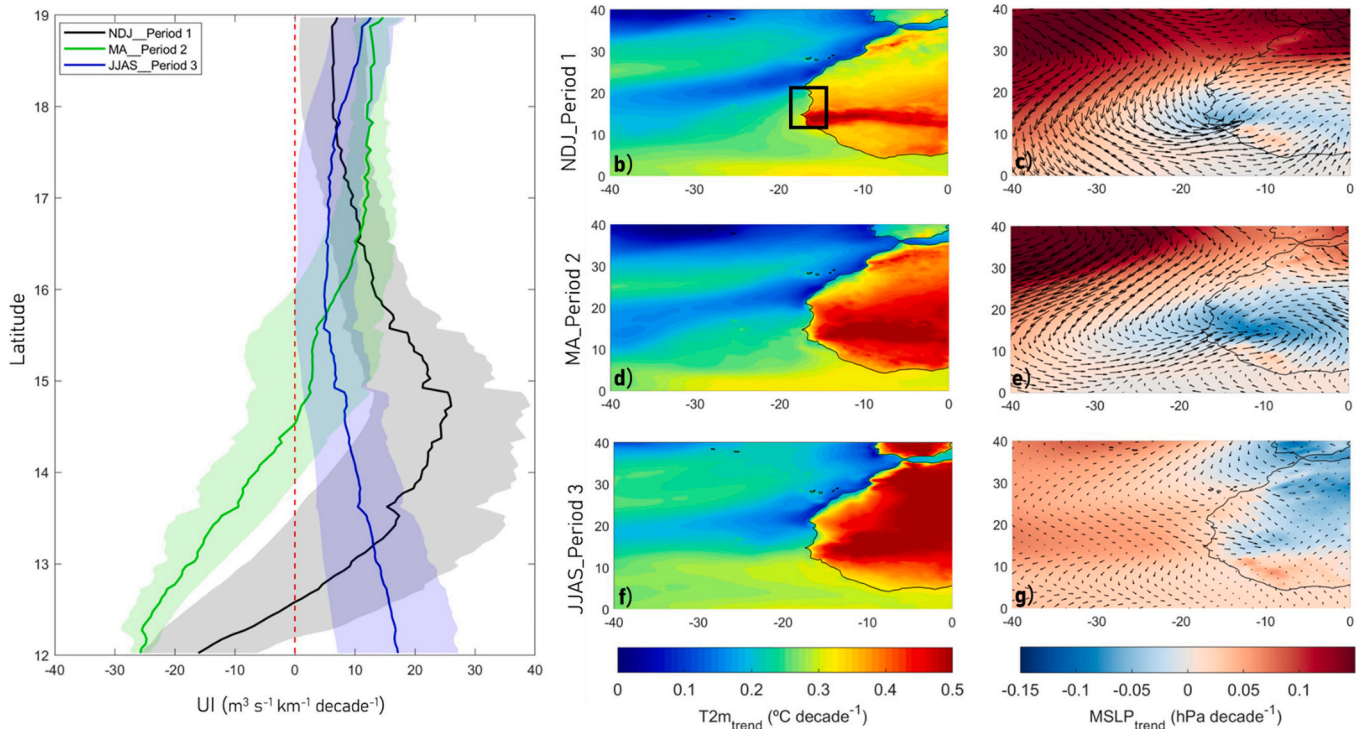


Fig. 5. *UI* trends (solid lines) and standard deviation (shading areas) averaged over the closest grid points to the coast from 1950 to 2099 for each period (a). *T2m* (b, d, f) and *MSLP* (c, e, g) trends averaged from 1950 to 2099 for each period. Wind differences between the last 30 years of ROM_P2 (2070–2099) and ROM_P1 (1976–2005) are represented over the *MSLP* trends for each period. The black box (b) represents the MSUR (12°N–19°N).

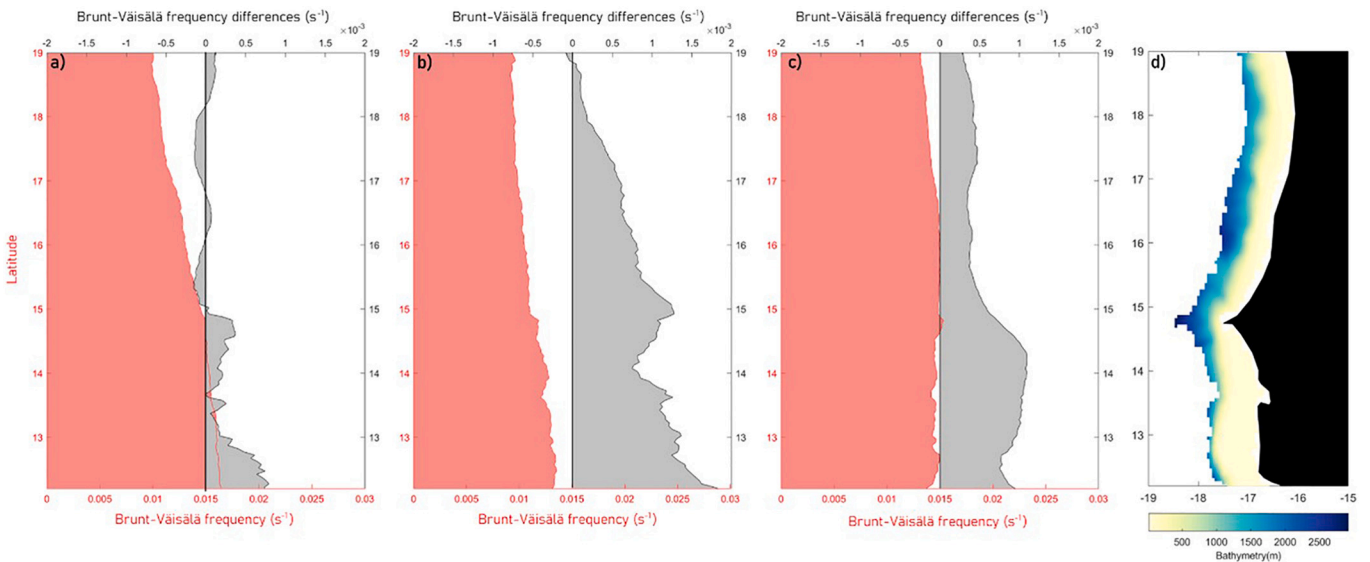


Fig. 6. Brunt-Väisälä frequency (s^{-1}) averaged from surface to 150 m in the closest grid points to coast for Period 1 (a), Period 2 (b) and Period 3 (c) for ROM_P1 (red shading; Historical) and the differences between ROM_P2 and ROM_P1 (grey shading; RCP8.5 - Historical). The mask used is shown in the panel d.

upwelling zone is already hampering the ascent of deeper water towards the surface, and [Sousa et al. \(2020\)](#) proposed the same hypothesis for the northern region of the Iberian upwelling. We found an enhanced ocean stratification in Period 2 (spring), very similar to the summer period (Period 3), associated with an increase in temperature in the ocean surface layers (Fig. S2). This pattern may be associated with a shorter and warmer spring seasons at the end of the century found in most CMIP5 models ([Wang et al., 2021](#)), resulting in an extended summer season throughout the year, except for the winter months (Period 1).

The combined effect of wind patterns and ocean stratification was

evaluated through the upwelling source water depth. In this regard, we found deeper water that upwells in Period 1 for the whole MSUR and in the northern MSUR for Period 2 due to the increase of wind effect (*UI*), and we found no differences when only the effect of stratification was considered (Fig. S5a). Conversely, in the southern MSUR the upwelling source water depth will be shallower for Period 2, where the decrease in *UI* along with the enhanced ocean stratification contributes to this shallowing of the upwelling source water depth (Fig. S5b). These results along with those recently reported by different authors (e.g. [Oyarzún and Brierley, 2019](#); [Sousa et al., 2020](#); [Chang et al., 2023](#); [Jing et al.,](#)

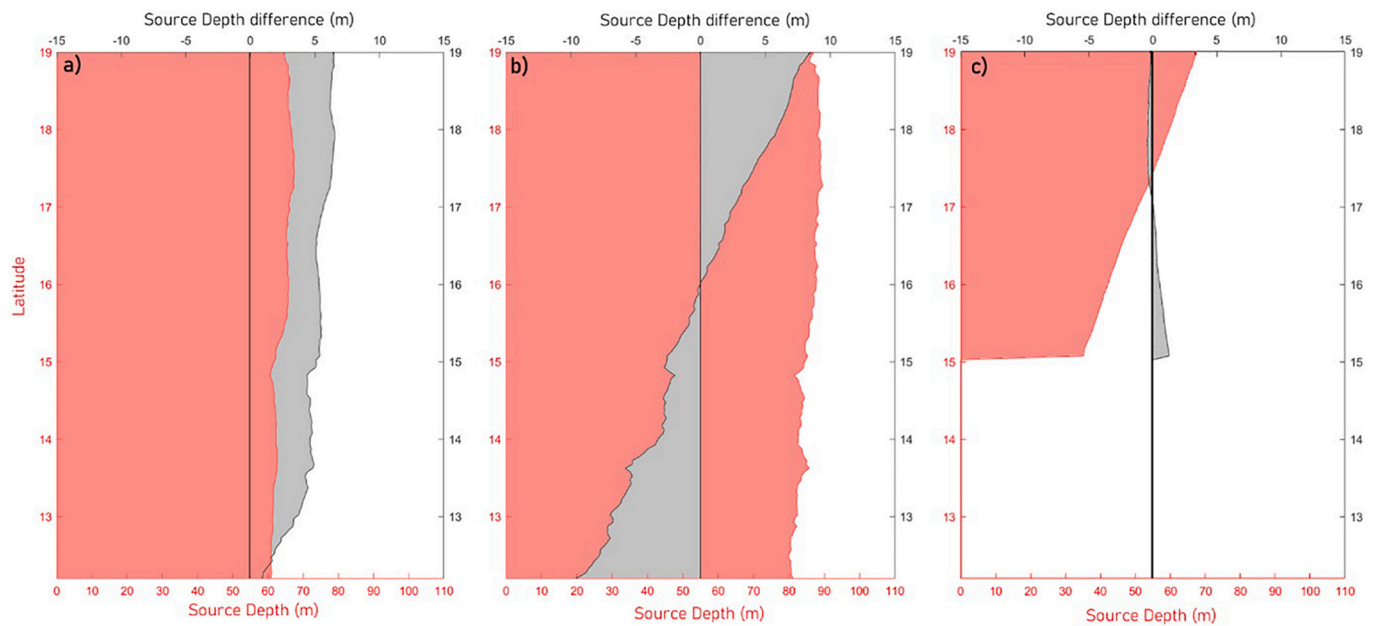


Fig. 7. Upwelling source water depth (m) in the closest grid points to coast (Fig. 6d) for Period 1 (a), Period 2 (b) and Period 3 (c) both for ROM_P1 (red shading; Historical) and the differences between ROM_P2 and ROM_P1 (grey shading; RCP8.5 - Historical). The mask used is shown in Fig. 6d.

2023) call on the need to evaluate the future evolution of upwelling systems at a larger resolution both latitudinally and monthly.

Finally, although the changes in the ocean stratification seem not to lead the upwelling changes in much of the MSUR, the ocean temperature increase is more than evident across the whole area. This fact may affect to the ecosystem balance in the MSUR, modifying the distribution of species, migrations and fisheries (Menge and Menge, 2013; Wang et al., 2015a; Wang et al., 2015b).

6. Conclusions

The objective of this work is to assess the MSUR under the RCP8.5 scenario, clarifying the effects of the climate change on the wind pattern and ocean stratification, as well as to explore the main mechanisms responsible for these changes. To this end, we take advantage of ROM RCM, which presents a high horizontal resolution in MSUR. Our findings can be summarized as follows:

- ROM reproduces well the seasonality of the alongshore favourable winds in a present time, as well as the main drivers of the wind patterns: Azores high and ITCZ.
- Under the RCP8.5 scenario, we found three responses of the wind pattern to climate change depending on seasonality: Intensification of favourable upwelling winds across the whole MSUR (January–November–December; Period 1); strengthening of upwelling favourable winds in the northern MSUR and weakening in the southern MSUR (March–April; Period 2); weak intensification of upwelling favourable winds in the northern MSUR and weakening of downwelling favourable winds in the southern MSUR (June–July–August–September; Period 3).
- These responses of the wind pattern to climate change are associated with a strengthening of the Azores High in Periods 1 and 2, but with the particularity that Period 1 presents a local increase in the T2m in the southern Sahel region. The wind pattern found under RCP8.5 scenario in Period 3 is associated with a drastic increase in the T2m field throughout the African continent.
- Ocean stratification will be increase in the MSUR under global warming conditions, primarily during Period 2, associated with a surface temperature increase.

- Finally, the combined effect of changes associated with the wind pattern and ocean stratification in MSUR reveal a deepening of the upwelling source water depth during Period 1 and in the northern MSUR for Period 2, and a shallowing of the upwelling source water depth in the southern MSUR during Period 2.

CRedit authorship contribution statement

R. Vázquez, A. Izquierdo and W. Cabos planned the study and designed the analysis framework. R. Vázquez processed data conducted the analysis and wrote the manuscript. D.V. Sein performed the ROM runs. I.M. Parras-Berrocal, S. Koseki, W. Cabos, D.V. Sein and A. Izquierdo contributed with the analysis performance and interpretation of the results. A. Izquierdo revised and edited the final version of the manuscript. R.Vázquez prepared everything.

Declaration of competing interest

The authors declare that they have no known competing financial interests or personal relationships that could have appeared to influence the work reported in this paper.

Data availability

Data will be made available on request.

Acknowledgement

R. Vázquez was supported through a doctoral grant at the University of Ferrara and University of Cádiz, the Spanish Ministry of Science, Innovation and Universities (I+D+I PID2021-128656OB-I00) and the Plan Propio UCA 2022-23. I. M. Parras-Berrocal was supported by the Spanish National Research Plan through project TRUCO (RTI2018-100865-B-C22) and the Plan Propio UCA 2022-23. W. Cabos was funded by the Alcalá University project (PIUAH21/CC-058) and the Spanish Ministry of Science, Innovation and Universities, through grant (I+D+I PID2021-128656OB-I00). D.V. Sein worked in the framework of the SIO RAS state assignment (FMWE-2021-0014) and was also supported by the Federal Ministry of Education and Research of Germany (BMBF) in the

framework of ACE project (grant O1LP2004A). Simulations were done at the German Climate Computing Center (DKRZ), granted by its Scientific Steering Committee (WLA) under project ID ba0987.

Appendix A. Supplementary data

Supplementary data to this article can be found online at <https://doi.org/10.1016/j.scitotenv.2023.166391>.

References

- Abrahams, A., Schlegel, R.W., Smit, A.J., 2021. Variation and change of upwelling dynamics detected in the world's eastern boundary upwelling systems. *Front. Mar. Sci.* 8, 626411.
- Aguirre, C., Rojas, M., Garreaud, R.D., et al., 2019. Role of synoptic activity on projected changes in upwelling-favourable winds at the ocean's eastern boundaries. *npj Clim. Atmos. Sci.* 2, 44. <https://doi.org/10.1038/s41612-019-0101-9>.
- Aristegui, J., Barton, E.D., Álvarez-Salgado, X.A., Santos, A.M.P., Figueiras, F.G., Kifani, S., Hernández-León, S., Mason, E., Machú, E., Demarcq, H., 2009. Sub-regional ecosystem variability in the canary current upwelling. *Prog. Oceanogr.* 83, 33–48. <https://doi.org/10.1016/j.pocean.2009.07.031>.
- Bakun, A., 1973. Coastal Upwelling Indices, West Coast of North America. 1946–71. US Department of Commerce, National Oceanic and Atmospheric Administration, National Marine Fisheries Service.
- Bakun, A., 1990. Global climate change and intensification of coastal ocean upwelling. *Science* 247, 198–201. <https://doi.org/10.1126/science.247.4939.198>.
- Barton, E.D., 1998. Eastern boundary of the North Atlantic: Northwest Africa and Iberia. *The global coastal ocean: regional studies and syntheses*. In: Robinson, A.R., Brink, K.H. (Eds.), *The Sea—Ideas and Observations on Progress in the Study of the Seas*, Vol. 11. John Wiley and Sons, pp. 633–657.
- Benazzou, A., Mordane, S., Orbi, A., Chagdali, M., Hilmi, K., Atillah, A., Pelegrí, J.L., Hervé, D., 2014. An improved coastal upwelling index from sea surface temperature using satellite-based approach—the case of the canary current upwelling system. *Cont. Shelf Res.* 81, 38–54. <https://doi.org/10.1016/j.csr.2014.03.012>.
- Benazzou, A., Demarcq, H., González-Nuevo, G., de Vigo, C.O., 2015. Recent changes and trends of the upwelling intensity in the canary current large marine ecosystem. *Oceanogr. Biol. Features Canary Curr. Large Mar. Ecosyst.* 115, 321–330. <https://doi.org/10.4060/ca7253en>.
- Bindoff, N.L., Cheung, W.W.L., Kairo, J.G., Aristegui, J., Guinder, V.A., Hallberg, R., Hilmi, N., Jiao, N., Karim, M.S., Levin, L., O'Donoghue, S., Purca Cuicapusa, S.R., Rinkevich, B., Suga, T., Tagliabue, A., Williamson, P., 2019. Changing ocean, marine ecosystems, and dependent communities. In: Pörtner, H.-O., Roberts, D.C., Masson-Delmotte, V., Zhai, P., Tignor, M., Poloczanska, E., Mintenbeck, K., Alegria, A., Nicolai, M., Okem, A., Petzold, J., Rama, B., Weyer, N.M. (Eds.), *IPCC Special Report on the Ocean and Cryosphere in a Changing Climate*.
- Bonino, G., Di Lorenzo, E., Masina, S., Iovino, D., 2019. Interannual to decadal variability within and across the major eastern boundary upwelling systems. *Sci. Rep.* 9, 1–14. <https://doi.org/10.1038/s41598-019-56514-8>.
- Capet, X.J., Marchesiello, P., McWilliams, J.C., 2004. Upwelling response to coastal wind profiles. *Geophys. Res. Lett.* 31 (13), 1–4. <https://doi.org/10.1029/2004GL020123>.
- Capet, X., Estrade, P., Machu, E., Ndoye, S., Grelet, J., Lazar, A., Mari, L., Dausse, D., Brehmer, P., 2017. On the dynamics of the southern Senegal upwelling center: observed variability from synoptic to superinterannual scales. *J. Phys. Oceanogr.* 47 (1), 155–180.
- Chang, P., Xu, G., Kurian, J., Small, R.J., Danabasoglu, G., Yeager, S., Castruccio, F., Zhang, Q., Rosenbloom, N., Chapman, P., 2023. Uncertain future of sustainable fisheries environment in eastern boundary upwelling zones under climate change. *Commun. Earth Environ.* 4, 19. <https://doi.org/10.1038/s43247-023-00681-0>.
- Cook, K.H., Vizy, E.K., 2015. Detection and analysis of an amplified warming of the Sahara Desert. *J. Clim.* 28 (16), 6560–6580. <https://doi.org/10.1175/JCLI-D-14-00230.1>.
- Cropper, T.E., Hanna, E., Bigg, G.R., 2014. Spatial and temporal seasonal trends in coastal upwelling off Northwest Africa, 1981–2012. *Deep Sea Res.* 86, 94–111. <https://doi.org/10.1016/j.dsr.2014.01.007>.
- Dee, D.P., Uppala, S.M., Simmons, A.J., Berrisford, P., Poli, P., Kobayashi, S., Andrae, U., Balmaseda, M.A., Balsamo, G., Bauer, P., Bechtold, P., Beljaars, A.C.M., van den Berg, L., Bidlot, J., Bormann, N., Delsol, C., Dragani, R., Fuentes, M., Geer, A.J., Haimberger, L., Healy, S.B., Hersbach, H., Hólm, E.V., Isaksen, I., Kallber, P., Köhler, M., Matricardi, M., McNally, A.P., Monge-Sanz, B.M., Morcrette, J.J., Park, B. K., Peubey, C., de Rosnay, P., Tavolato, C., Thépaut, J.N., Vitart, F., 2011. The ERA-interim reanalysis: configuration and performance of the data assimilation system. *Q. J. R. Meteor. Soc.* 137, 553–597. <https://doi.org/10.1002/qj.828>.
- Fox-Kemper, B., Ferrari, R., Hallberg, R., 2008. Parameterization of mixed layer eddies. Part I: theory and diagnosis. *J. Phys. Oceanogr.* 38 (6), 1145–1165. <https://doi.org/10.1175/2007JPO3792.1>.
- García-Reyes, M., Sydeman, W.J., Schoeman, D.S., Ryzkaczewski, R.R., Black, B.A., Smit, A.J., Bograd, S.J., 2015. Under pressure: climate change, upwelling, and eastern boundary upwelling ecosystems. *Front. Mar. Sci.* 2, 109. <https://doi.org/10.3389/fmars.2015.00109>.
- Giorgetta, M.A., Jungclaus, J., Reick, C.H., Legutke, S., Bader, J., Böttinger, M., Brovkin, V., Crueger, T., Esch, M., Fieg, K., Glushak, K., Gayler, V., Haak, H., Hollweg, H.D., Ilyina, T., Kinne, S., Kornbluh, L., Matei, D., Mauritsen, T., Mikolajewicz, U., Mueller, W., Notz, D., Pithan, F., Raddatz, T., Rast, S., Redler, R., Roeckner, E., Schmidt, H., Schnur, R., Segsneider, J., Six, K.D., Stockhause, M., Timmreck, C., Wegner, J., Widmann, H., Wieners, K.H., Claussen, M., Marotzke, J., Stevens, B., 2013. Climate and carbon cycle changes from 1850 to 2100 in MPI-ESM simulations for the coupled model Intercomparison project phase 5. *J. Adv. Model Earth Syst.* 5, 572–597. <https://doi.org/10.1002/jame.20038>.
- Gómez-Letona, M., Ramos, A.G., Coca, J., Aristegui, J., 2017. Trends in primary production in the canary current upwelling system a regional perspective comparing remote sensing models. *Front. Mar. Sci.* 4, 370. <https://doi.org/10.3389/fmars.2017.00370>.
- Haarsma, R.J., Roberts, M.J., Vidale, P.L., Senior, C.A., Bellucci, A., Bao, Q., Chang, P., Corti, S., Fučkar, N.S., Guemas, V., von Hardenberg, J., Hazeleger, W., Kodama, C., Koenigk, T., Leung, L.R., Lu, J., Luo, J.-J., Mao, J., Mizielinski, M.S., Mizuta, R., Nobre, P., Satoh, M., Scoccimarro, E., Semmler, T., Small, J., von Storch, J.-S., 2016. High Resolution Model Intercomparison Project (HighResMIP v1.0) for CMIP6. *Geosci. Model Dev.* 9, 4185–4208. <https://doi.org/10.5194/gmd-9-4185-2016>.
- Hagemann, S., Dumenil-Gates, L., 1998. A parameterization of the lateral waterflow for the global scale. *Clim. Dyn.* 14, 17–31. <https://doi.org/10.1007/s003820050205>.
- Hagemann, S., Dumenil-Gates, L., 2001. Validation of the hydrological cycle of ECMWF and NCEP reanalysis using the MPI hydrological discharge model. *J. Geophys. Res.* 106 (D2), 1503–1510. <https://doi.org/10.1029/2000JD900568>.
- He, J., Mahadevan, A., 2021. How the source depth of coastal upwelling relates to stratification and wind. *J. Geophys. Res. Oceans* 126 (12), e2021JC017621. <https://doi.org/10.1029/2021JC017621>.
- Hersbach, H., Bell, B., Berrisford, P., Hirahara, S., Horanyi, A., Muñoz-Sabater, J., Nicolas, J., Peubey, C., Radu, R., Schepers, D., Simmons, A., Soci, C., Abdalla, S., Abellan, X., Balsamo, G., Bechtold, P., Biavati, G., Bidlot, J., Bonavita, M., Thépaut, J.N., 2020. The ERA5 global reanalysis. *Q. J. R. Meteorol. Soc.* 146 (730), 1999–2049. <https://doi.org/10.1002/qj.3803>.
- Hibler, W.D., 1979. A dynamic thermodynamic sea ice model. *J. Phys. Oceanogr.* 9, 815–846.
- Ikazaki, K., 2015. Desertification and a new countermeasure in the Sahel, West Africa. *Soil Sci. Plant Nutr.* 61, 372–383. <https://doi.org/10.1080/00380768.2015.1025350>.
- Izquierdo, A., Mikolajewicz, U., 2019. The role of tides in the spreading of Mediterranean outflow waters along the southwestern Iberian margin. *Ocean Model* 133, 27–43. <https://doi.org/10.1016/j.ocemod.2018.08.003>.
- Jacob, D., 2001. A note to the simulation of the annual and interannual variability of the water budget over the Baltic Sea drainage basin. *Meteorol. Atmos. Phys.* 77 (1–4), 61–73. <https://doi.org/10.1007/s007030170017>.
- Jacox, M.G., Edwards, C.A., Hazen, E.L., Bograd, S.J., 2018. Coastal upwelling revisited: Ekman, Bakun, and improved upwelling indices for the U.S. West Coast. *J. Geophys. Res. Oceans* 123, 7332–7350. <https://doi.org/10.1029/2018JC014187>.
- Jing, Z., Wang, S., Wu, L., Wang, H., Zhou, S., Sun, B., Chen, Z., Ma, X., Gan, B., Yang, H., 2023. Geostrophic flows control future changes of oceanic eastern boundary upwelling. *Nat. Clim. Chang.* 13, 148–154. <https://doi.org/10.1038/s41558-022-01588-y>.
- Kämpf, J., Chapman, P., 2016. The canary/Iberia current upwelling system. In: *Upwelling Systems of the World*, pp. 203–250. https://doi.org/10.1007/978-3-319-42524-5_6.
- Kirichek, A., 1971. Water circulation in the north-eastern part of the tropical Atlantic. *Internat. Council. Explor. Sea. CM* 100, 7.
- Klenz, T., Dengler, M., Brandt, P., 2018. Seasonal variability of the Mauritanian undercurrent and hydrography at 18° N. *J. Geophys. Res. Oceans* 123, 8122–8137. <https://doi.org/10.1029/2018JC014264>.
- Kounta, L., Capet, X., Jouanno, J., Kolodziejczyk, N., Sow, B., Gaye, A.T., 2018. A model perspective on the dynamics of the shadow zone of the eastern tropical North Atlantic. Part I: the poleward slope currents along West Africa. *Ocean Sci.* 14 (5), 971–997. <https://doi.org/10.5194/os-14-971-2018>.
- Lathuilière, C., Echevin, V., Lévy, M., 2008. Seasonal and intraseasonal surface chlorophyll-a variability along the northwest African coast. *J. Geophys. Res.* 113, C05007. <https://doi.org/10.1029/2007JC004433>.
- Levitus, S., Boyer, T.P., Conkright, M.E., O'Brien, T., Antonov, J., Stephens, C., Stathopoulos, L., Johnson, D., Gelfeld, R., 1998. *World ocean database 1998*. In: *Introduction, NOAA Atlas NESDIS 18, Ocean Clim. Lab., Natl. Oceanogr. Data Cent., U.S. Gov. Print. Off., Washington, D.C.*, vol. 1.
- Lovecchio, E., Gruber, N., Münnich, M., Lachkar, Z., 2017. On the longrange offshore transport of organic carbon from the canary upwelling system to the open North Atlantic. *Biogeosciences* 14 (13), 3337–3369. <https://doi.org/10.3929/ethz-b-000190480>.
- Marsland, S.J., Haak, H., Jungclaus, J.H., Latif, M., Roeske, F., 2003. The max-Planck-institute global ocean/sea icemodel with orthogonal curvilinear coordinates. *Ocean Model* 5 (2), 91–127. [https://doi.org/10.1016/S1463-5003\(02\)00015-X](https://doi.org/10.1016/S1463-5003(02)00015-X).
- Menge, B.A., Menge, D.N.L., 2013. Dynamics of coastal meta-ecosystems: the intermittent upwelling hypothesis and a test in rocky intertidal regions. *Ecol. Monogr.* 83, 283–310.
- Merchant, C.J., Embury, O., Bulgin, C.E., Block, T., Corlett, G., Fiedler, E., Good, S.A., Mittaz, J., Rayner, N., Berry, D., Eastwood, S., 2019. Satellite-based time-series of sea-surface temperature since 1981 for climate applications. *Nat. Sci. Data* 6, 223. <https://doi.org/10.1038/s41597-019-0236-x>.
- Mignot, J., Mejia, C., Sorror, C., Sylla, A., Crépon, M., et al., 2020. Towards an objective assessment of climate multi-model ensembles - a case study: the Senegalo-Mauritanian upwelling region. *Geosci. Model Dev.* 13 (6), 2723–2742. [https://doi.org/10.5194/gmd-13-2723-2020off\(fhhal-02889987f\)](https://doi.org/10.5194/gmd-13-2723-2020off(fhhal-02889987f)).
- Ndoye, S., Capet, X., Estrade, P., Sow, B., Machu, E., Brochier, T., Döring, J., Brehmer, P., 2017. Dynamics of a “low-enrichment high-retention” upwelling center over the

- southern Senegal shelf. *Geophys. Res. Lett.* 44 (10), 5034–5043. <https://doi.org/10.1002/2017GL072789>.
- Oerder, V., Colas, F., Echevin, V., Codron, F., Tam, J., Belmadani, A., 2015. Peru-Chile upwelling dynamics under climate change. *J. Geophys. Res. Oceans* 120 (2), 1152–1172. <https://doi.org/10.1002/2014JC010102>, 99.
- Oyarzún, D., Brierley, C.M., 2019. The future of coastal upwelling in the Humboldt current from model projections. *Clim. Dyn.* 52, 599–615. <https://doi.org/10.1007/s00382-018-4158-7>.
- Pardo, P.C., Padín, X.A., Gilcoto, M., Farina-Busto, L., Pérez, F.F., 2011. Evolution of upwelling systems coupled to the long-term variability in sea surface temperature and Ekman transport. *Clim. Res.* 48 (2–3), 231–246. <https://doi.org/10.3354/cr00989>.
- Peña-Izquierdo, J., Pelegrí, J.L., Pastor, M.V., Castellanos, P., Emelianov, M., Gasser, M., Salvador, J., VázquezDomínguez, E., 2012. The continental slope current system between Cape Verde and the Canary Islands. *Sci. Mar.* 76, 65–78. <https://doi.org/10.3989/scimar.03607.18C>.
- Rykaczewski, R.R., Dunne, J.P., Sydeman, W.J., Garcia-Reyes, M., Black, B.A., Bograd, S. J., 2015. Poleward displacement of coastal upwelling-favorable winds in the ocean's eastern boundary currents through the 21st century. *Geophys. Res. Lett.* 42, 6424–6431. <https://doi.org/10.1002/2015GL064694>.
- Santana-Falcón, Y., Mason, E., Arístegui, J., 2020. Offshore transport of organic carbon by upwelling filaments in the canary current system. *Prog. Oceanogr.* 184 (April), 102322. <https://doi.org/10.1016/j.pocean.2020.102322>.
- Sein, D.V., Mikolajewicz, U., Gröger, M., Fast, I., Cabos, W., Pinto, J.G., Hagemann, S., Semmler, T., Izquierdo, A., Jacob, D., 2015. Regionally coupled atmosphere-ocean-sea ice-marine biogeochemistry model ROM: 1. Description and validation. *J. Adv. Model Earth Sy* 7, 268–304. <https://doi.org/10.1002/2014MS000357>.
- Sein, D.V., Koldunov, N.V., Danilov, S., Wang, Q., Sidorenko, D., Fast, I., Rackow, T., Cabos, W., Jung, T., 2017. Ocean modeling on a mesh with resolution following the local rossby radius. *J. Adv. Model E Sys* 9, 2601–2614. <https://doi.org/10.1002/2017MS001099>.
- Soares, P.M.M., Lima, D.C.A., Semedo, A., et al., 2019. Assessing the climate change impact on the North African offshore surface wind and coastal low-level jet using coupled and uncoupled regional climate simulations. *Clim. Dyn.* 52, 7111–7132. <https://doi.org/10.1007/s00382-018-4565-9>.
- Sousa, M.C., de Castro, M., Álvarez, I., Gomez-Gesteira, M., Dias, J.M., 2017a. Why coastal upwelling is expected to increase along the Western Iberian Peninsula over the next century? *Sci. Total Environ.* 592, 243–251. <https://doi.org/10.1016/j.scitotenv.2017.03.046>.
- Sousa, M.C., Alvarez, I., deCastro, M., Gomez-Gesteira, M., Dias, J.M., 2017b. Seasonality of coastal upwelling trends under future warming scenarios along the southern limit of the canary upwelling system. *Prog. Oceanogr.* 153, 16–23. <https://doi.org/10.1016/j.pocean.2017.04.002>.
- Sousa, M.C., Ribeiro, A., Des, M., Gomez-Gesteira, M., deCastro, M., Dias, J.M., 2020. NW Iberian Peninsula coastal upwelling future weakening: competition between wind intensification and surface heating. *Sci. Total Environ.* 703, 134808.
- Stramma, L., 1984. Geostrophic transport in the warm water sphere of the eastern subtropical North Atlantic. *J. Mar. Res.* 42 (3), 537–558. <https://doi.org/10.1357/002224084788506022>.
- Sylla, A., Mignot, J., Capet, X., Gaye, A.T., 2019. Weakening of the Senegalo-Mauritanian upwelling system under climate change. *Clim. Dyn.* 53 (7–8), 4447–4473. <https://doi.org/10.1007/s00382-019-04797-y>.
- Sylla, A., Sanchez Gomez, E., Mignot, J., López-Parages, J., 2022. Impact of increased resolution on the representation of the Canary upwelling system in climate models. *Geosci. Model Dev.* 15, 8245–8267. <https://doi.org/10.5194/gmd-15-8245-2022>.
- Valcke, S., 2013. The OASIS3 coupler: a European climate modelling community software. *Geosci. Model Dev.* 6, 373–388. <https://doi.org/10.5194/gmd-6-373-2013>.
- Varela, R., Alvarez, I., Santos, F., deCastro, M., Gomez-Gesteira, M., 2015. Has upwelling strengthened along worldwide coasts over 1982–2010? *Sci. Rep.* 0016 doi:10.1038/srep1. <https://doi.org/10.1038/srep1>.
- Varela, R., Rodríguez-Díaz, L., de Castro, M., Gómez-Gesteira, M., 2022. Influence of canary upwelling system on coastal SST warming along the 21st century using CMIP6 GCMs. *Glob. Planet. Chang.* 208, 103692.
- Vázquez, R., Parras-Berrocal, I., Cabos, W., Sein, D.V., Mañanes, R. and Izquierdo, A. (2022). Assessment of the canary current upwelling system in a regionally coupled climate model. *Clim. Dyn.* 58, 69–85. <https://doi.org/10.1007/s00382-021-05890-x>.
- Vélez-Belchí, P., PedroCañinos, V., Romero, E., Pérez-Hernández, M.D., Hernández-Guerra, A., Santana-Toscano, D., González-Santana, A., Pérez-Hernández, M.D., Hernández-Guerra, A., 2021. The canary intermediate poleward undercurrent: not another poleward undercurrent in an eastern boundary upwelling system. *J. Phys. Oceanogr.* 51, 2973–2990. <https://doi.org/10.1175/jpo-d-20-0130.1>.
- Wang, Y., Castela, R.M., Yuan, Y., 2015a. Seasonal variability of alongshore winds and sea surface temperature fronts in eastern boundary current systems. *J. Geophys. Res. Oceans* 120 (3), 2385–2400.
- Wang, D.W., Gouhier, T.C., Menge, B.A., Ganguly, A.R., 2015b. Intensification and spatial homogenization of coastal upwelling under climate change. *Nature* 518. <https://doi.org/10.1038/nature14235>.
- Wang, J., Guan, Y., Wu, L., Guan, X., Cai, W., Huang, J., Dong, W., Zhang, B., 2021. Changing lengths of the four seasons by global warming. *Geophys. Res. Lett.* 48. <https://doi.org/10.1029/2020GL091753>.
- Xiu, P., Chai, F., Curchitser, E., Castruccio, F., 2018. Future changes in coastal upwelling ecosystems with global warming: the case of the California current system. *Sci. Rep.* 8, 2866. <https://doi.org/10.1038/s41598-018-21247-7>.
- Zhou, L.M., 2016. Desert amplification in a warming climate. *Sci. Rep.* 6 (ARTN3106510.1038/srep31065).